GEOPHYSICS, VOL. 74, NO. 2 (MARCH-APRIL 2009); P. I1–I7, 5 FIGS.
10.1190/1.3073761

General line integrals for gravity anomalies of irregular 2D masses with horizontally and vertically dependent density contrast

Xiaobing Zhou[1]

ABSTRACT

Line integrals (LIs) are an efficient tool in calculating the gravity anomaly caused by an irregular 2D mass body because the 2D surface integral is reduced to a 1D LI. Historically, LIs have been derived for 2D mass bodies of depth-dependent density contrast. I derive LIs for 2D mass bodies with density contrast dependent on (1) horizontal and (2) horizontal and vertical directions. Assuming the density contrast depends only on horizontal position, two types of representative LIs are derived: LIs with logarithmic kernel and density-integrated LIs for any integrable density-contrast function. A general density-contrast model that depends on horizontal and vertical directions is developed to include three components: a function of horizontal position, a function of vertical position, and a sum of crossterms of horizontal and vertical positions. Based on the general density-contrast model defined and proper selection of 2D vector gravity potentials, general LIs are derived to calculate the gravity anomaly. The newly developed LI method is then compared with two cases from the literature in calculating gravity anomaly, and agreement is obtained. However, the new LI method allows for more general 2D density-contrast variations and can be used to calculate the gravity anomaly of a 2D mass body. Such a mass body can have any cross-sectional profile that can be approximated by a polygonal cross section with any density-contrast function that can be approximated by a rich set of basis functions.

INTRODUCTION

Dimensional reduction in the computational domain in forward modeling or inversion in geophysical exploration is an efficient way for a fast solution. In principle, the gravity anomaly caused by a 2D mass with any density-contrast function can be computed via a numerical surface integral. Converting a 2D areal integral to 1D line integrals (LIs) in gravity anomaly calculations can reduce the computational time significantly, except for cases in which the cross section of the mass body is very elongated or when all of the integrations can be performed analytically (e.g., Pohánka, 1988, 1998; Hansen, 1999; Holstein, 2003). Generally, when a 2D areal integral is reduced to a 1D LI, a surface with an order of N^2 internally discretized elementary grids can be expected to have an order of N boundary elements. The number of integration steps can be reduced from an order of N^2 to an order of N. Thus, a reduction by an order of N in computational time can be expected by using the LI method. The gain arises from reducing a numerical areal integral to a sum of numerical LIs. This reduction is significant, making the LI method efficient and attractive.

To rapidly calculate gravity anomalies caused by a 2D mass of complex geometry and variable density contrast using the LI method, defining the LIs is the key starting point. Historically, LIs have been obtained for 2D masses of constant or depth-dependent density contrast (Hubbert, 1948; Murthy and Rao, 1979; Zhou, 2008). Hubbert (1948) obtains an LI for 2D masses of constant density for calculating gravity anomaly, the foundation for Talwani et al.'s (1959) classic computational scheme for rapid computation of gravity resulting from irregular 2D masses when the mass density is constant. Murthy and Rao (1979) extend Hubbert's LI to cases when the mass density contrast is a function of depth.

Using Stokes' theorem and the right-hand rule in converting a 2D areal integral for gravity anomaly to a 1D LI, Zhou (2008) defines a 2D vector gravity potential. Based on the nonuniqueness characteristics of the 2D vector gravity potential for a specific problem, he defines two types of LIs for computing gravity anomalies because of 2D masses of complex geometry and depth-dependent density contrast. The first type is LIs with arctangent kernel for any density-contrast function in depth. The second type is density-integrated LIs with algebraic kernel when the density-contrast function is integrable. As shown by Zhou (2008), these LIs are computationally efficient in gravity anomaly calculations that involve a depth-dependent density contrast of very broad interest (Cordell, 1973; Murthy and

Manuscript received by the Editor 16 June 2008; revised manuscript received 7 November 2008; published online 20 February 2009.
[1]Montana Tech of the University of Montana, Department of Geophysical Engineering, Butte, Montana, U.S.A. E-mail: xzhou@mtech.edu.

Rao, 1979; Rao, 1986; Chai and Hinze, 1988; Litinsky, 1989; Rao et al., 1990; García-Abdeslem, 1992; Rao et al., 1994; Pohánka, 1998; Hansen, 1999; Holstein, 2003; García-Abdeslem et al., 2005; Silva et al., 2006; Chakravarthi and Sundararajan, 2007; Chappell and Kusznir, 2008).

However, the density contrast of earth material also can be dependent on horizontal position or on horizontal and vertical positions (Gendzwill, 1970; Cordell, 1979; Pan, 1989; Ruotoistenmäki, 1992; Martín-Atienza and García-Abdeslem, 1999; Zhang et al., 2001). For gravity anomaly calculation at the surface, intrusions or folded sedimentary units could have an arbitrary density function in the horizontal direction and a polynomial density distribution in the vertical direction. On the other hand, dipping layered intrusions or sedimentary beds could have an arbitrary density function of depth and a polynomial function of horizontal coordinates (Ruotoistenmäki, 1992).

The objective of this paper is to derive LIs for geological problems in which the density contrast depends on horizontal or on horizontal and vertical directions. First, a general density model that encompasses a broad range of geologic settings is to be developed. Based on the general density-contrast model, proper 2D vector gravity potentials are selected. The gravity anomaly is defined as the LIs of the components of the 2D vector gravity potentials along the contour of an irregular mass body. Because LIs for such problems have not yet been studied, the LIs derived for a 2D irregular mass body with any density-contrast function that can be approximated by a rich set of basis functions will be very useful in rapid computation of gravity anomaly. Then, applications of these general LIs to gravity anomaly calculations for a broad range of geological settings will be discussed.

GENERAL DENSITY-CONTRAST MODEL FOR 2D MASS BODIES

In 2D gravity anomaly calculations, most past studies consider the density contrast as a constant (e.g., Bott, 1960; Corbató, 1965; Pohánka, 1988; Ferguson et al., 1988; Litinsky, 1989), as a function of depth only (Cordell, 1973; Murthy and Rao, 1979; Rao, 1986; Chai and Hinze, 1988; Litinsky, 1989; D. B. Rao et al., 1990; García-Abdeslem, 1992; C. V. Rao et al., 1994; García-Abdeslem et al., 2005; Silva et al., 2006; Chakravarthi and Sundararajan, 2007; Chappell and Kusznir, 2008), or as a unidirectional function in 3D (Pohánka, 1998; Hansen, 1999; Holstein, 2003). The dependence of density contrast on depth is primarily because of mechanical compaction and diagenesis resulting in reduced porosity and thus is of general interest (Guspí, 1990; Zhang et al., 2001; Chappell and Kusznir, 2008).

There also are several studies considering the density contrast as a function of horizontal coordinates or as a function of horizontal and vertical positions (Gendzwill, 1970; Cordell, 1979; Pan, 1989; Ruotoistenmäki, 1992; Martín-Atienza and García-Abdeslem, 1999; Zhang et al., 2001). Cordell (1979) proposes that lateral variations can be caused by fan development, with the absolute value of density contrast increasing toward the center of the basin. Vertically layered intrusives can have a density-contrast function varying horizontally. The reason is that vertically homogeneous rocks can be metamorphosed, so there is a gradual horizontal change in density between two rock types (Gendzwill, 1970; Ruotoistenmäki, 1992). On some occasions, the density contrast in such a density transition zone can be approximated as horizontally linear (Gendzwill, 1970; Pan, 1989). Pan (1989) uses a linear horizontal density-contrast model to estimate the depth of a sedimentary basin adjacent to the master fault associated with the Rio Grande rift in New Mexico. The surface density contrast may vary significantly within a relatively short horizontal distance because of the differing lithological character of the rocks forming various parts of the surface topography, or it may change considerably even within the same sand body if part of it is cemented to sandstone (Vajk, 1956). For dipping layered intrusions or sedimentary beds, the density may vary horizontally. For all of these cases, the density is often modeled as a polynomial function of horizontal coordinate x (Ruotoistenmäki, 1992), with the linear function as a special case.

In some areas, different rock types are separated by interbedding, intrusive rocks such as plutons characterized by lit-par-lit structures at their contacts. Steeply dipping sequences of beds and long-term contact metamorphism result in density changes. In these cases, the density contrast is often modeled as piecewise continuous functions of x (Pan, 1989; Ruotoistenmäki, 1992).

Complicated geologic and geochemical processes in the diagenesis of rocks, such as nonuniform stratification, physical and chemical cementations, volcanic eruptions and structural disruptions, and heterogeneous metamorphisms, often cause the density distribution to be more complicated than a simple function of one dimension, forcing us to consider an arbitrary variation of density contrast in gravity anomaly modeling (Martín-Atienza and García-Abdeslem, 1999; Zhang et al., 2001). To accommodate a broad variety of geologic formations, I consider the following density-contrast model as a general case:

$$\Delta\rho(x,z) = h(x) + v(z) + \sum_{j=1}^{N_x}\sum_{k=1}^{N_z} D_{jk}\xi_j(x)\eta_k(z). \quad (1)$$

The first and second terms in equation 1 describe the components of the density contrast that depend only on horizontal x and vertical z directions, respectively. The third term describes a sum of crossterms of the density contrast that depends on horizontal and vertical positions. Index $j = 1,2,\ldots,N_x$, and $k = 1,2,\ldots,N_z$. The values N_x and N_z are the number of functions that depend only on x and z, respectively; D_{jk} is the coefficient of each crossterm. If the first and third terms in equation 1 are zero, the general density-contrast model degenerates to the depth-dependent model, the LIs of which are studied systematically by Zhou (2008). If the second and third terms are zero, the general model degenerates to the horizontal-position-dependent model, the LIs of which are derived in the next section. If $\xi_j(x) = x^j$ and $\eta_k(z) = z^k$ in the third term of equation 1, it represents a polynomial function that is usually a least-squares fit to the density logging data, a special case studied by Zhang et al. (2001).

LIs FOR DENSITY CONTRAST VARYING WITH HORIZONTAL POSITION

Consider the geometry of a 2D mass body (Figure 1) that is infinitely long in the y-direction and whose mass density contrast is a general function of x and z. The vertical component of gravity anomaly at point $P(x_i,0)$ is

$$g_z(x_i,0) = 2G\iint_S \frac{\Delta\rho(x,z)z}{(x-x_i)^2+z^2}dxdz, \quad (2)$$

where G is Newton's gravitational constant. This is the general form of a 2D areal integral for calculating gravity anomaly at any point

$P(x_i,0)$ along the x-axis because of 2D masses with density contrast varying horizontally in x and vertically in z.

LIs with logarithmic kernel

Let us first consider the cases where the density contrast is only a function of horizontal position, i.e., $\Delta\rho = h(x)$. By definition, a 2D vector potential $\mathbf{A}$ satisfies (Zhou, 2008)

$$\frac{\partial A_x}{\partial z} - \frac{\partial A_z}{\partial x} = \frac{2Gh(x)z}{(x-x_i)^2+z^2}, \tag{3}$$

so the vertical component of gravity anomaly caused by a 2D mass becomes

$$g_z(x_i,0) = \oint_C (A_x dx + A_z dz). \tag{4}$$

Equation 4 means that the gravity anomaly caused by a 2D mass is equal to the net circulation of the 2D vector gravity potential $\mathbf{A}$ along the closed contour C bounding the mass. Let me choose the 2D vector gravity potential $\mathbf{A}$ that satisfies equation 3 as follows:

$$\begin{cases} A_x = Gh(x)\ln[(x-x_i)^2+z^2] \\ A_z = 0 \end{cases}. \tag{5}$$

Inserting equation 5 in equation 4, the vertical component of the gravity anomaly becomes

$$g_z(x_i,0) = \oint_C \mathbf{A}\cdot d\mathbf{l} = G\oint_C h(x)\ln[(x-x_i)^2+z^2]dx, \tag{6}$$

where $d\mathbf{l}$ is a differential length along contour C. Equation 6 is called an LI with logarithmic kernel for density contrast varying with horizontal position because it contains a logarithmic function in its integrand. The counterpart of the LI with a logarithmic kernel for the horizontally dependent model is an LI with arctangent kernel for the depth-dependent density-contrast model, studied by Zhou (2008). The LIs with a logarithmic kernel have not been studied but are direct results of defining a 2D vector gravity potential (Zhou, 2008). When $\Delta\rho = \Delta\rho_0$, equation 6 becomes Hubbert's LI (Hubbert, 1948), as it does for the depth-dependent case (Zhou, 2008), because both represent the same constant density-contrast model.

LIs with algebraic kernel

Assume that the density-contrast function $\Delta\rho = h(x)$ is integrable. Let me define a density-contrast integral as

$$F(x) = \frac{1}{x-x_i}\int h(x)dx + C_0, \tag{7}$$

so that

$$F(x)' = \frac{dF(x)}{dx} = \frac{\Delta\rho(x) - F(x)}{x-x_i}. \tag{8}$$

The value C_0 in equation 7 is a constant that is independent of x for a specific density-contrast model. We can prove that

$$\frac{\partial}{\partial z}\left[\frac{2GF(x)z^2}{(x-x_i)^2+z^2}\right] - \frac{\partial}{\partial x}\left[-\frac{2G(x-x_i)F(x)z}{(x-x_i)^2+z^2}\right] = \frac{2Gh(x)z}{(x-x_i)^2+z^2}. \tag{9}$$

Comparing equation 9 with equation 3, I obtain a 2D vector gravity potential $\mathbf{A}$ as follows:

$$\begin{cases} A_x = 2G\dfrac{F(x)z^2}{(x-x_i)^2+z^2} \\ A_z = -2G\dfrac{(x-x_i)F(x)z}{(x-x_i)^2+z^2} \end{cases}. \tag{10}$$

Inserting equation 10 in equation 4, the gravity anomaly becomes

$$g_z(x_i,0) = 2G\oint_C\left(\frac{F(x)z^2}{(x-x_i)^2+z^2}dx - \frac{(x-x_i)F(x)z}{(x-x_i)^2+z^2}dz\right). \tag{11}$$

Equation 11 is called an LI with algebraic kernel for the horizontal density-contrast model.

GENERAL LIs

Now let me consider the general density-contrast model (equation 1). The first term in equation 1 is for the horizontal density-contrast model, the LIs of which have been obtained in the above section. The second term is for the depth-dependent model, the LIs of which are studied systematically by Zhou (2008). The only LIs that need to be found are for the crossterms. Consider the general crossterm $D_{jk}\xi_j(x)\zeta_k(z)$, where $\xi_j(x)$ is any function of x and $\zeta_k(z)$ is any function of z. We define the integrals for $\xi_j(x)$ and $\zeta_k(z)$ as follows:

$$\Xi_j(x,z) = \int \frac{\xi_j(x)}{(x-x_i)^2+z^2}dx, \tag{12}$$

$$Z_k(x,z) = \int \frac{z\zeta_k(z)}{(x-x_i)^2+z^2}dz. \tag{13}$$

The 2D vector gravity potential corresponding to the general crossterm $D_{jk}\xi_j(x)\zeta_k(z)$ is denoted as $\mathbf{A}_{jk}$, satisfying

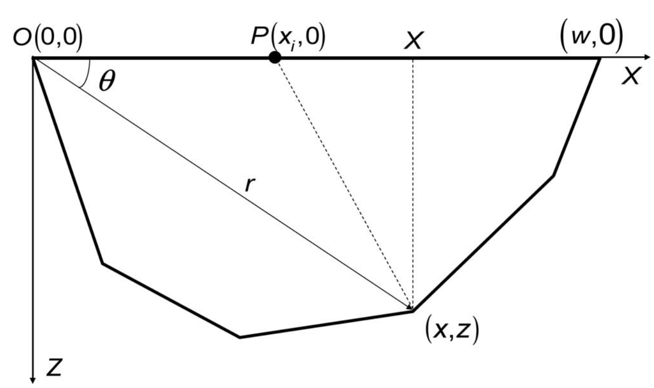

Figure 1. The 2D cross section of a sedimentary basin, where w is the width of the basin.

$$\frac{\partial A_{jk,x}}{\partial z} - \frac{\partial A_{jk,z}}{\partial x} = \frac{2GD_{jk}\xi_j(x)z\zeta_k(z)}{(x-x_i)^2+z^2}. \qquad (14)$$

If the integration in equation 13 is easier to perform than that in equation 13, I choose $\mathbf{A}_{jk}$ as follows:

$$\begin{cases} A_{jk,x} = 0 \\ A_{jk,z} = -2GD_{jk}\Xi_j(x,z)z\zeta_k(z) \end{cases}. \qquad (15)$$

Otherwise, I choose $\mathbf{A}_{jk}$ as

$$\begin{cases} A_{jk,x} = 2GD_{jk}\xi_j(x)Z_k(x,z) \\ A_{jk,z} = 0 \end{cases}. \qquad (16)$$

By the superposition principle, for the general density-contrast model, the total 2D vector gravity potential is the vector addition of the depth-dependent term (Zhou, 2008), the horizontal term (equation 5), and the crossterms (equation 15), i.e.,

$$\begin{cases} A_x = Gh(x)\ln\left[(x-x_i)^2+z^2\right] \\ A_z = -2G\left[v(z)\arctan\left(\dfrac{x-x_i}{z}\right) + \displaystyle\sum_{j=1}^{N_x}\sum_{k=1}^{N_y} D_{jk}\Xi_j(x,z)z\zeta_k(z)\right]. \end{cases} \qquad (17)$$

Inserting equation 17 in equation 4, the gravity anomaly becomes

$$\begin{aligned} g_z(x_i,0) = {} & G\oint_C h(x)\ln\left[(x-x_i)^2+z^2\right]dx \\ & - 2G\oint_C\left[v(z)\arctan\left(\frac{x-x_i}{z}\right) + \sum_{j=1}^{N_x}\sum_{k=1}^{N_y} D_{jk}\Xi_j(x,z)z\zeta_k(z)\right]dz. \end{aligned} \qquad (18)$$

If $Z_j(x,z)$ is easier to obtain than $\Xi_j(x,z)$, the counterpart of equation 17 is

$$\begin{aligned} g_z(x_i,0) = {} & G\oint_C\left\{h(x)\ln\left[(x-x_i)^2+z^2\right] + 2\sum_{j=1}^{N_x}\sum_{k=1}^{N_y} D_{jk}\xi_j(x)Z_k(x,z)\right\}dx \\ & - 2G\oint_C\left[v(z)\arctan\left(\frac{x-x_i}{z}\right)\right]dz. \end{aligned} \qquad (19)$$

Here, the 2D vector gravity potential (equation 17) is based on the criterion that the number of integrals contained in the LIs must be at a minimum to save computation time. This means that (1) for the density-contrast component $v(z)$, which depends on depth, the arctangent function (Zhou, 2008) is chosen; (2) for the density-contrast component $h(x)$, which depends only on horizontal position, the logarithmic function (equation 4) is chosen; and (3) for the crossterms $D_{jk}\xi_j(x)\zeta_k(z)$, which depend on horizontal and vertical positions, the 2D vector gravity potential associated with $\Xi_j(x,z)$ (equation 15) or that associated with $Z_k(x,z)$ (equation 16) is chosen. Therefore, equations 18 and 19 are called general LIs for the general density-contrast model (equation 1). The general LIs (equations 18 and 19) include an LI with arctangent kernel and equation 6 as special cases when the general density-contrast model degenerates to the vertical and horizontal models, respectively.

Further analytical (closed-form) solution or numerical calculation of gravity anomaly is then based on the LIs, depending on the exact form of the density-contrast function. If the density-contrast function is a simple function such as a polynomial function, an analytical solution is possible (Zhang et al., 2001); otherwise, a numerical solution must be found.

APPLICATION OF GENERAL LIs

For numerical calculations, the contour of a 2D mass body is usually modeled as a polygon, with each segment or side of the polygon being a line segment unless the exact form of the contour equation is known. The number of vertices or segments of the contour bounding the mass is assumed to be M (in Figure 1, $M=6$). The nth segment is formed from points (x_n,z_n) and (x_{n+1},z_{n+1}) in counterclockwise order, the line equation of which is given in parametric form as (Zhou, 2008)

$$x = x_n(1-t) + x_{n+1}t, \quad z = z_n(1-t) + z_{n+1}t \qquad (20)$$

and

$$dx = (x_{n+1}-x_n)dt, \quad dz = (z_{n+1}-z_n)dt, \qquad (21)$$

where t is a parameter between 0 and 1. This parameterized form for the mass boundary has the added advantage that the interval [0,1] for t is adapted easily for Gaussian quadrature. Thus, equation 18 becomes

$$\begin{aligned} g_z(x_i,0) = {} & G\sum_{n=1}^{M}\int_{x_n}^{x_{n+1}} h(x)\ln\left[(x-x_i)^2+z^2\right]dx \\ & - 2G\sum_{n=1}^{M}\int_{z_n}^{z_{n+1}}\left[v(z)\arctan\left(\frac{x-x_i}{z}\right) + \sum_{j=1}^{N_x}\sum_{k=1}^{N_y} D_{jk}\Xi_j(x)z\zeta_k(z)\right]dz. \end{aligned} \qquad (22)$$

For the numerical integration of each segment, the Gauss-Legendre quadrature method (Zhou et al., 2003) is used to conduct the integrations in equation 22. Because the abscissas and weights of the k-point Gauss-Legendre quadrature formula are based on the interval $(-1,1)$, the actual integration interval for each segment of the polygonal cross section is transformed into the $(-1,1)$ range (Davis and Rabinowitz, 1984).

In principle, the LIs of equations 18 and 19 apply to any 2D mass problems with any density-contrast function that can be expressed in the form of equation 1. In the following discussion, some complicated density-contrast model functions are used to show that the LI method can handle not only complex geometry with simple 2D density-contrast functions but also with sophisticated 2D density-contrast models.

Case studies with density contrast varying with horizontal position

For the problems with a density contrast depending only on the horizontal position, the gravity anomaly is calculated using the LI with logarithmic kernel (equation 6) or the LI with algebraic kernel (equation 11).

Figure 2a shows the geometry of a mass body with density contrast dependent only on horizontal position x as follows (Martín-Atienza and García-Abdeslem, 1999):

$$\Delta\rho = h(x) = 0.5 + 2\times10^{-5}x - 2\times10^{-8}x^2, \quad (23)$$

where $\Delta\rho = h(x)$ is in grams per cubic centimeter and x is in meters. Figure 2b shows the gravity anomaly. The number of nodes for Gaussian quadrature is $k = 20$. The results calculated at 41 stations using equation 22 agree well with those by Martín-Atienza and García-Abdeslem (1999). The analytic and numerical methods as described by Martín-Atienza and García-Abdeslem (1999) require the top and bottom surfaces of the contour of the mass body to be parallel to the x-axis, or the left and right surfaces to be parallel to the z-axis. The LI method (equation 18 and 19) does not require any special requirement of the geometry of the mass body. Compared with the case shown in Figure 2, Figure 3a shows the geometry of a more complicated irregular mass body with the density contrast dependent only on the horizontal position x but in a more sophisticated way as follows:

$$\Delta\rho = h(x) = 0.7 + 1.2e^{-|0.001x-5|} - 30\frac{x}{x^2+1000}. \quad (24)$$

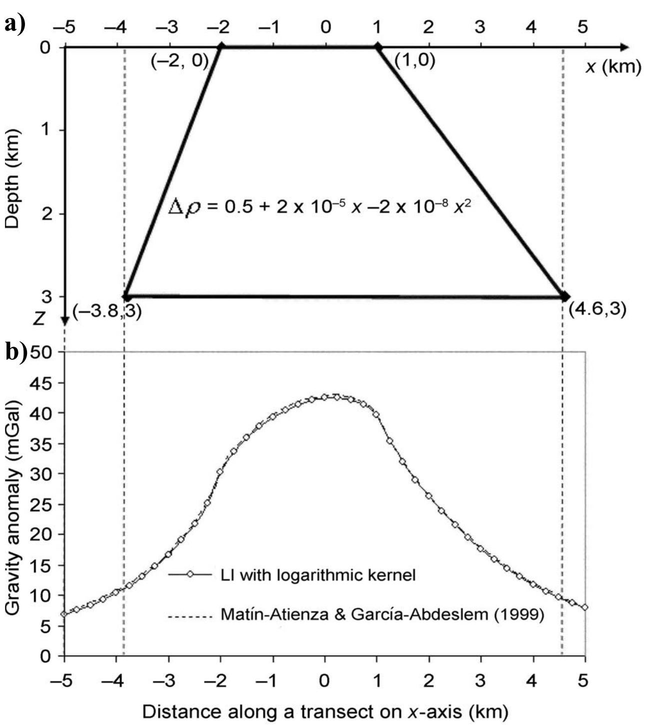

Figure 2. (a) Simple geometry of a 2D mass body with density contrast dependent only on the horizontal position x: $\Delta\rho = h(x) = 0.5 + 2\times10^{-5}x - 2\times10^{-8}x^2$. (b) Gravity anomaly calculated using the LI with logarithmic kernel. The results by Martín-Atienza and García-Abdeslem (1999) also are shown for comparison.

The contour of the mass body is approximated as a 90-segment polygon, in which case 90 segments are chosen so that no segment is longer than 1 km and average segment length is 350 m. The gravity anomalies at 49 stations are calculated. Figure 3b shows the gravity anomaly and the x-distribution of density contrast. This example demonstrates the capability of the LIs (equation 18 and 19) in handling any irregular mass body and complicated dependence of the density contrast on the horizontal position. From Figure 3b, we can see that the position of maximum gravity anomaly does not coincide with that of the peak density contrast, indicating the asymmetry of the mass source.

Case studies with density contrast varying in horizontal and vertical directions

For the problems with density contrast varying with horizontal and vertical positions, the gravity anomaly is calculated using the general LIs (equation 18 and 19). Figure 4a shows the geometry of the irregular mass body studied by Martín-Atienza and García-Abdeslem (1999), representing folded and overturned strata in a sedimentary basin. The density contrast varies in horizontal and vertical directions:

$$\Delta\rho(x,z) = -0.7 - 5\times10^{-8}xz + 4\times10^{-8}x^2 + 6\times10^{-8}z^2. \quad (25)$$

The main difference between this density-contrast model and that in Figure 3 is the crossterm. Set $h(x) = 4\times10^{-8}x^2$, $v(z) = -0.7 + 6\times10^{-8}z^2$, $N_x = N_z = 1$, $D_{11} = -5\times10^{-8}$, $\xi_1(x) = x$, and $\zeta_1(z) = z$. The value $\Xi_1(x,z)$ is found from equation 12 as $\Xi_1(x,z) = (1/2)\ln[(x-x_i)^2 + z^2] + (x_i/z)\tan^{-1}((x-x_i)/z)$. The boundary

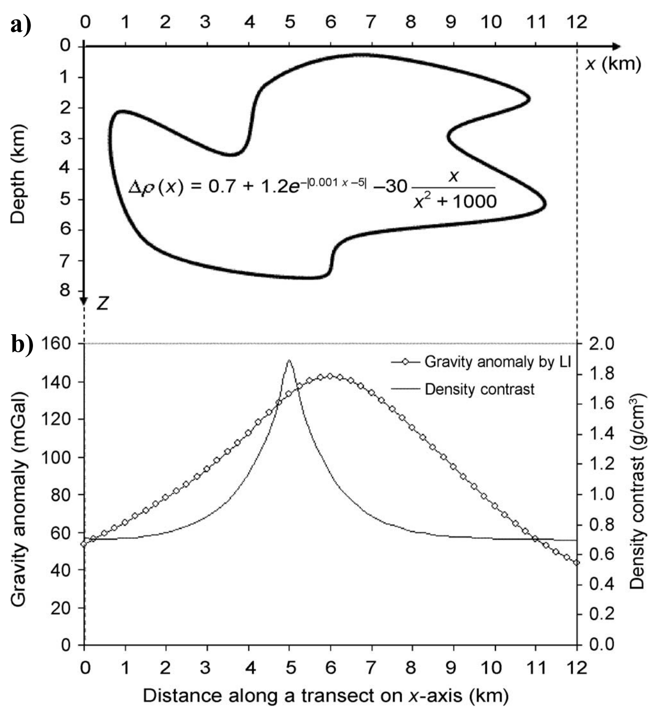

Figure 3. (a) Geometry of a 2D irregular mass body with density contrast dependent only on horizontal position x: $\Delta\rho = h(x) = 0.7 + 1.2e^{-|0.001x-5|} - 30(x/x^2 + 1000)$. (b) Gravity anomaly calculated using the LI with a logarithmic kernel.

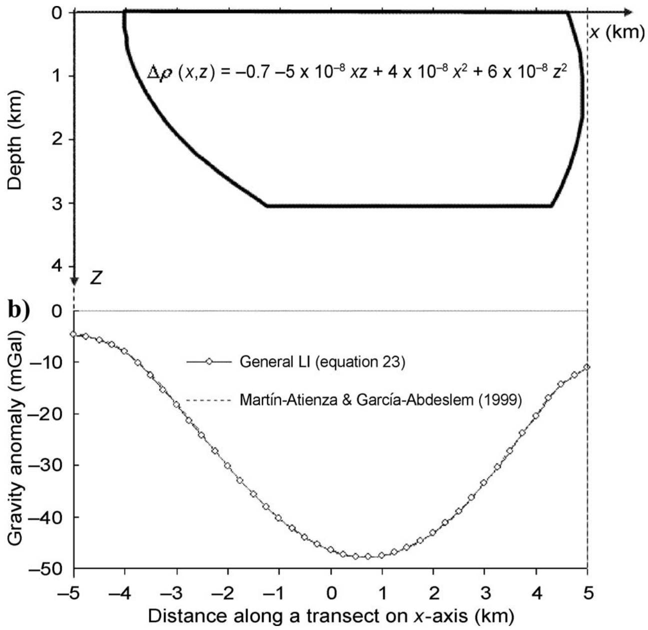

Figure 4. (a) Geometry of a 2D mass body with density contrast dependent on horizontal and vertical positions: $\Delta\rho(x,z) = -0.7 - 5\times10^{-8}xz + 4\times10^{-8}x^2 + 6\times10^{-8}z^2$. (b) Gravity anomaly calculated using the general LI equation 18. Results by Martín-Atienza and García-Abdeslem (1999) also are shown for comparison.

a)
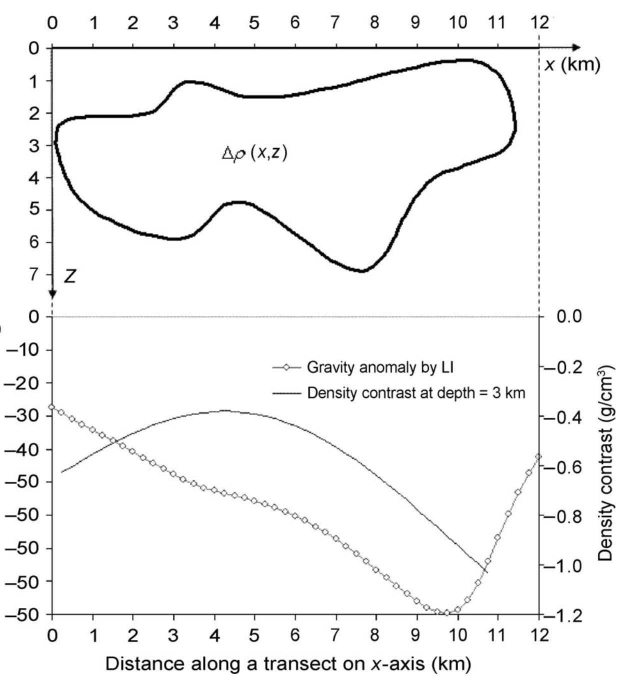

Figure 5. (a) The 2D cross section of an exhumed sedimentary basin with a distorted top surface. The density contrast varies with horizontal and vertical positions in a sophisticated way: $\Delta\rho(x,z) = -0.77 + 0.46\cos(0.0003x - 1.5) - 1.1e^{-5.1\times10^{-4}z} + 1090e^{-1.2\times10^{-4}x}(z/(z^2 + 2\times10^6))$. (b) The gravity anomaly calculated using the general LI equation 19.

of the 2D mass is approximated as a 26-segment polygon. Figure 4b shows the gravity anomalies at 41 stations calculated using equation 21. For comparison, the results by Martín-Atienza and García-Abdeslem (1999) also are shown. The results using the general LI method agree very well with those by Martín-Atienza and García-Abdeslem (1999).

Figure 5a shows the geometry of an exhumed sedimentary basin with a distorted top surface. No single-value functions can be used to describe the boundary. The mass density contrast is

$$\begin{aligned}\Delta\rho(x,z) &= -0.77 + 0.46\cos(0.0003x - 1.5) \\ &\quad - 1.1e^{-5.1\times10^{-4}z} \\ &\quad + 1090e^{-1.2\times10^{-4}x}\frac{z}{z^2 + 2\times10^6},\end{aligned}\tag{26}$$

where z is in meters. Set $h(x) = 0.46\cos(0.0003x - 1.5)$, $v(z) = -0.77 - 1.1e^{-5.1\times10^{-4}z}$, $N_x = N_z = 1$, $D_{11} = 1090$, $\xi_1(x) = e^{-1.2\times10^{-4}x}$, and $\zeta_1(z) = z/(z^2 + 2\times10^6)$. For this case, finding $Z_1(x,z)$ from equation 13 is easier than finding $\Xi_1(x,z)$ from equation 12:

$$\begin{aligned}Z_1(x,z) &= \frac{1}{(x-x_i)^2 - 2\times10^6}\left\{|x-x_i|\arctan\left(\frac{z}{|x-x_i|}\right)\right. \\ &\quad \left. - \sqrt{2}\times10^3\arctan\left(\frac{z}{\sqrt{2}\times10^3}\right)\right\}.\end{aligned}\tag{27}$$

Thus, the LI of equation 19 is used to find the gravity anomaly. The contour of the 2D mass body is approximated as a 109-segment polygon.

Figure 5b shows the gravity anomalies at 49 stations calculated using equation 18 and the x-profile of density contrast at a depth $z = 3$ km. This example demonstrates the capability of the general LIs (equation 18 and 19) in calculating gravity anomaly because of any irregular mass body and the sophisticated dependence of the density contrast on horizontal and vertical positions. The advantage of using the general LIs is that no restriction on the irregularity is imposed.

CONCLUSIONS

Based on the concept of a 2D vector gravity potential, LIs with a logarithmic kernel and LIs with an algebraic kernel for density contrast dependent only on horizontal position are obtained. A general density-contrast model that depends on horizontal and vertical directions has been developed. General LIs are thus based on the general density-contrast model and the proper selection of 2D vector gravity potentials. The general LIs degenerate to the LIs with a logarithmic kernel (horizontal) and the LIs with an arctangent kernel (vertical) when the general density-contrast model degenerates to the horizontal and vertical models, respectively. Comparison of the gravity anomaly calculated using the general LIs with other methods indicates the general LIs work excellently. Besides, the new LI method allows for more general 2D density-contrast variations.

The general LI method works very well for an irregular mass body that can be approximated as a polygon with any density-contrast function in which all crossterms can be expressed as products of basic mathematical functions of x and z. Otherwise, the general LI algorithm does not work. For instance, if the density-contrast function includes any crossterm such as $\sin(xz)$ or $\cos(xz)$, the LI method will not work. This is because $\sin(xz)$ or $\cos(xz)$ cannot be separated into products of basic trigonometry functions of x and z so that the density-contrast function can be cast into the form of equation 1. If the density contrast depends only on one dimension, either x or z, the LI algorithm works very well for any form of the 1D density-contrast function.

The 2D vector gravity potential is useful in finding LI for calculating the gravity anomaly of a 2D mass body of irregular geometry and with density contrast varying either in horizontal, vertical, or horizontal and vertical directions. In addition, the general LIs developed provide an efficient algorithm for fast computation of gravity anomaly because of any 2D mass body with any density-contrast function that can be cast into the form of the general density-contrast model. Thus, the LI method is very useful in gravity anomaly modeling and interpretation for a broad range of geologic settings.

ACKNOWLEDGMENTS

Thanks go to Horst Holstein, Rao Yalamanchili, an anonymous reviewer, associate editor John W. Peirce, assistant editor Steven A. Arcone, and editor Kees Wapenaar for their very helpful comments and suggestions. Thanks also go to Leif Cox (Montana Tech of the University of Montana) for helpful comments that improved the readability of the manuscript.

REFERENCES

Bott, M. H. P., 1960, The use of rapid digital computing methods for direct gravity interpretation of sedimentary basins: Geophysical Journal of the Royal Astronomical Society, **3**, 63–67.

Chai, Y., and W. J. Hinze, 1988, Gravity inversion of an interface above which the density contrast varies exponentially with depth: Geophysics, **53**, 837–845.

Chakravarthi, V., and N. Sundararajan, 2007, 3D gravity inversion of basement relief — A depth-dependent density approach: Geophysics, **72**, no. 2, I23–I32.

Chappell, A., and N. Kusznir, 2008, An algorithm to calculate the gravity anomaly of sedimentary basins with exponential density-depth relationships: Geophysical Prospecting, **56**, 249–258.

Corbató, C. E., 1965, A least-squares procedure for gravity interpretation: Geophysics, **30**, 228–233.

Cordell, L., 1973, Gravity analysis using an exponential density-depth function — San Jacinto Graben, California: Geophysics, **38**, 684–690.

———, 1979, Sedimentary facies and gravity anomaly across master faults of the Rio Grande rift in New Mexico: Geology, **7**, 201–205.

Davis, P. J., and P. Rabinowitz, 1984, Methods of numerical integration, 2nd ed.: Academic Press Inc.

Ferguson, J. F., R. N. Felch, C. L. V. Aiken, J. S. Oldow, and H. Dockery, 1988, Models of the Bouguer gravity and geologic structure at Yucca Flat, Nevada: Geophysics, **53**, 231–244.

García-Abdeslem, J., 1992, Gravitational attraction of a rectangular prism with depth-dependent density: Geophysics, **57**, 470–473.

García-Abdeslem, J., J. M. Romo, E. Gómez-Treviño, J. Ramírez-Hernández, F. J. Esparza-Hernández, and C. F. Flores-Luna, 2005, A constrained 2D gravity model of the Sebastián Vizcaíno Basin, Baja California Sur, Mexico: Geophysical Prospecting, **53**, 755–765.

Gendzwill, D. J., 1970, The gradational density contrast as a gravity interpretation model: Geophysics, **35**, 270–278.

Guspí, F., 1990, General 2D gravity inversion with density contrast varying with depth: Geoexploration, **26**, 253–265.

Hansen, R. O., 1999, An analytical expression for the gravity field of a polyhedral body with linearly varying density: Geophysics, **64**, 75–77.

Holstein, H., 2003, Gravimagnetic anomaly formulas for polyhedra of spatially linear media: Geophysics, **68**, 157–167.

Hubbert, M. K., 1948, A line-integral method of computing the gravimetric effects of two-dimensional masses: Geophysics, **13**, 215–225.

Litinsky, V. A., 1989, Concept of effective density: Key to gravity depth determinations for sedimentary basins: Geophysics, **54**, 1474–1482.

Martín-Atienza, B., and J. García-Abdeslem, 1999, 2-D gravity modeling with analytically defined geometry and quadratic polynomial density functions: Geophysics, **64**, 1730–1734.

Murthy, I. V. R., and D. B. Rao, 1979, Gravity anomalies of two dimensional bodies of irregular cross-section with density contrast varying with depth: Geophysics, **44**, 1525–1530.

Pan, J.-J., 1989, Gravity anomalies of irregularly shaped two-dimensional bodies with constant horizontal density gradient: Geophysics, **54**, 528–530.

Pohánka, V., 1988, Optimum expression for computation of the gravity field of a homogeneous polyhedral body: Geophysical Prospecting, **36**, 733–751.

———, 1998, Optimum expression for computation of the gravity field of a polyhedral body with linearly increasing density: Geophysical Prospecting, **46**, 391–404.

Rao, C. V., V. Chakravarthi, and M. L. Raju, 1994, Forward modelling: Gravity anomalies of two-dimensional bodies of arbitrary shape with hyperbolic and parabolic density functions: Computers and Geosciences, **20**, 873–880.

Rao, D. B., 1986, Modelling of sedimentary basins from gravity anomalies with variable density contrast: Geophysical Journal of the Royal Astronomical Society, **84**, 207–212.

Rao, D. B., M. J. Prakash, and N. Ramesh Babu, 1990, 3D and $2\frac{1}{2}$D modeling of gravity anomalies with variable density contrast: Geophysical Prospecting, **38**, 411–422.

Ruotoistenmäki, T., 1992, The gravity anomaly of two-dimensional sources with continuous density distribution and bounded by continuous surfaces: Geophysics, **57**, 623–628.

Silva, J. B. C., D. C. L. Costa, and V. C. F. Barbosa, 2006, Gravity inversion of basement relief and estimation of density contrast variation with depth: Geophysics, **71**, no. 5, J51–J58.

Talwani, M., J. L. Worzel, and M. Landisman, 1959, Rapid gravity computations for two-dimensional bodies with application to the Mendocino submarine fracture zone: Journal of Geophysical Research, **64**, 49–59.

Vajk, R., 1956, Bouguer corrections with varying surface density: Geophysics, **21**, 1004–1020.

Zhang, J., B. Zhong, X. Zhou, and Y. Dai, 2001, Gravity anomalies of 2D bodies with variable density contrast: Geophysics, **66**, 809–813.

Zhou, X., 2008, 2D vector gravity potential and line integrals for the gravity anomaly caused by a 2D mass of depth-dependent density contrast: Geophysics, **73**, no. 6, I43–I50.

Zhou, X., S. Li, and K. Stamnes, 2003, Geometrical-optics code for computing the optical properties of large dielectric spheres: Applied Optics, **42**, 4295–4306.